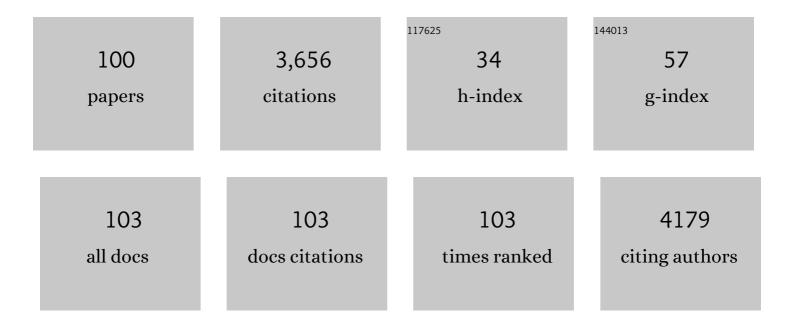
## Michael L Neidig

List of Publications by Year in descending order

Source: https://exaly.com/author-pdf/3496800/publications.pdf Version: 2024-02-01



#	Article	IF	CITATIONS
1	Characterization Methods for Paramagnetic Organometallic Complexes. , 2022, , 135-175.		1
2	A TMEDA–Iron Adduct Reaction Manifold in Ironâ€Catalyzed C(sp <sup>2</sup> )â^'C(sp <sup>3</sup> ) Crossâ€Coupling Reactions. Angewandte Chemie - International Edition, 2022, 61, .	13.8	4
3	Anion-induced disproportionation of Th( <scp>iii</scp> ) complexes to form Th( <scp>ii</scp> ) and Th( <scp>iv</scp> ) products. Chemical Communications, 2022, 58, 5289-5291.	4.1	5
4	Side-on coordination of diphosphorus to a mononuclear iron center. Science, 2022, 375, 1393-1397.	12.6	9
5	<i>C</i> -Term magnetic circular dichroism (MCD) spectroscopy in paramagnetic transition metal and f-element organometallic chemistry. Dalton Transactions, 2021, 50, 416-428.	3.3	10
6	Experimental and computational studies of the mechanism of iron-catalysed C–H activation/functionalisation with allyl electrophiles. Chemical Science, 2021, 12, 9398-9407.	7.4	10
7	C H Activation/Functionalization With Earth Abundant 3d Transition Metals. , 2021, , 260-310.		1
8	Activation of ammonia and hydrazine by electron rich Fe( <scp>ii</scp> ) complexes supported by a dianionic pentadentate ligand platform through a common terminal Fe( <scp>iii</scp> ) amido intermediate. Chemical Science, 2021, 12, 2231-2241.	7.4	21
9	Forged in iron. Nature Reviews Chemistry, 2021, 5, 223-224.	30.2	2
10	[2Fe–2S] Cluster Supported by Redox-Active <i>o</i> -Phenylenediamide Ligands and Its Application toward Dinitrogen Reduction. Inorganic Chemistry, 2021, 60, 13811-13820.	4.0	12
11	Additive and Counterion Effects in Iron-Catalyzed Reactions Relevant to C–C Bond Formation. ACS Catalysis, 2021, 11, 8493-8503.	11.2	22
12	Dilithium Amides as a Modular Bis-Anionic Ligand Platform for Iron-Catalyzed Cross-Coupling. Organic Letters, 2021, 23, 5958-5963.	4.6	4
13	NHC Effects on Reduction Dynamics in Ironâ€Catalyzed Organic Transformations**. Chemistry - A European Journal, 2021, 27, 13651-13658.	3.3	2
14	Near-infrared <i>C</i> -term MCD spectroscopy of octahedral uranium( <scp>v</scp> ) complexes. Dalton Transactions, 2021, 50, 5483-5492.	3.3	2
15	Air-Stable Iron-Based Precatalysts for Suzuki–Miyaura Cross-Coupling Reactions between Alkyl Halides and Aryl Boronic Esters. Organic Process Research and Development, 2021, 25, 2461-2472.	2.7	10
16	General method for iron-catalyzed multicomponent radical cascades–cross-couplings. Science, 2021, 374, 432-439.	12.6	53
17	Recent Advances in Synthesis, Characterization and Reactivities of Iron-Alkyl and Iron-Aryl Complexes. , 2021, , .		0
18	Intermediates and mechanism in iron-catalyzed C–H methylation with trimethylaluminum. Chemical	4.1	2

#	Article	IF	CITATIONS
19	Creation of an unexpected plane of enhanced covalency in cerium(III) and berkelium(III) terpyridyl complexes. Nature Communications, 2021, 12, 7230.	12.8	11
20	Ligand effects on electronic structure and bonding in U( <scp>iii</scp> ) coordination complexes: a combined MCD, EPR and computational study. Dalton Transactions, 2020, 49, 14401-14410.	3.3	12
21	The Exceptional Diversity of Homoleptic Uranium–Methyl Complexes. Angewandte Chemie, 2020, 132, 13688-13692.	2.0	1
22	Syntheses and characterizations of iron complexes of bulky <i>o</i> -phenylenediamide ligand. Dalton Transactions, 2020, 49, 12287-12297.	3.3	5
23	The Exceptional Diversity of Homoleptic Uranium–Methyl Complexes. Angewandte Chemie - International Edition, 2020, 59, 13586-13590.	13.8	16
24	TMEDA in Ironâ€Catalyzed Hydromagnesiation: Formation of Iron(II)â€Alkyl Species for Controlled Reduction to Alkeneâ€Stabilized Iron(0). Angewandte Chemie - International Edition, 2020, 59, 17070-17076.	13.8	14
25	TMEDA in Ironâ€Catalyzed Hydromagnesiation: Formation of Iron(II)â€Alkyl Species for Controlled Reduction to Alkeneâ€Stabilized Iron(0). Angewandte Chemie, 2020, 132, 17218-17224.	2.0	4
26	Insight into the Electronic Structure of Formal Lanthanide(II) Complexes using Magnetic Circular Dichroism Spectroscopy. Organometallics, 2019, 38, 3124-3131.	2.3	16
27	Identification and Reactivity of Cyclometalated Iron(II) Intermediates in Triazole-Directed Iron-Catalyzed C–H Activation. Journal of the American Chemical Society, 2019, 141, 12338-12345.	13.7	39
28	Homoleptic Aryl Complexes of Uranium (IV). Angewandte Chemie, 2019, 131, 10372-10376.	2.0	4
29	Atom-Economical Ni-Catalyzed Diborylative Cyclization of Enynes: Preparation of Unsymmetrical Diboronates. Organic Letters, 2019, 21, 6552-6556.	4.6	26
30	Isolation and Characterization of a Homoleptic Tetramethylcobalt(III) Distorted Square-Planar Complex. Organometallics, 2019, 38, 3486-3489.	2.3	1
31	The Effect of βâ€Hydrogen Atoms on Iron Speciation in Crossâ€Couplings with Simple Iron Salts and Alkyl Grignard Reagents. Angewandte Chemie, 2019, 131, 2795-2799.	2.0	16
32	Mechanism of the Bis(imino)pyridine-Iron-Catalyzed Hydromagnesiation of Styrene Derivatives. Journal of the American Chemical Society, 2019, 141, 10099-10108.	13.7	30
33	Homoleptic Aryl Complexes of Uranium (IV). Angewandte Chemie - International Edition, 2019, 58, 10266-10270.	13.8	24
34	Terminal coordination of diatomic boron monofluoride to iron. Science, 2019, 363, 1203-1205.	12.6	50
35	Development and Evolution of Mechanistic Understanding in Iron-Catalyzed Cross-Coupling. Accounts of Chemical Research, 2019, 52, 140-150.	15.6	92
36	The Effect of βâ€Hydrogen Atoms on Iron Speciation in Crossâ€Couplings with Simple Iron Salts and Alkyl Grignard Reagents. Angewandte Chemie - International Edition, 2019, 58, 2769-2773.	13.8	41

#	Article	IF	CITATIONS
37	Synthesis and characterization of a sterically encumbered homoleptic tetraalkyliron(III) ferrate complex. Polyhedron, 2019, 158, 91-96.	2.2	2
38	Crystal structure of bromidopentakis(tetrahydrofuran-ΰ <i>O</i> )magnesium bis[1,2-bis(diphenylphosphanyl)benzene-ΰ <sup>2</sup> <i>P</i> , <i>P</i> ′]cobaltate(â^'1) tetrahydrofuran disolvate. Acta Crystallographica Section E: Crystallographic Communications, 2019, 75, 304-307.	0.5	1
39	The <i>N</i> â€Methylpyrrolidone (NMP) Effect in Ironâ€Catalyzed Crossâ€Coupling with Simple Ferric Salts and MeMgBr. Angewandte Chemie - International Edition, 2018, 57, 6496-6500.	13.8	64
40	NHC and nucleophile chelation effects on reactive iron(ii) species in alkyl–alkyl cross-coupling. Chemical Science, 2018, 9, 1878-1891.	7.4	28
41	The <i>N</i> â€Methylpyrrolidone (NMP) Effect in Ironâ€Catalyzed Crossâ€Coupling with Simple Ferric Salts and MeMgBr. Angewandte Chemie, 2018, 130, 6606-6610.	2.0	19
42	Combined Effects of Backbone and N-Substituents on Structure, Bonding, and Reactivity of Alkylated Iron(II)-NHCs. Organometallics, 2018, 37, 3093-3101.	2.3	16
43	Intermediates and Mechanism in Iron-Catalyzed Cross-Coupling. Journal of the American Chemical Society, 2018, 140, 11872-11883.	13.7	79
44	A Pseudotetrahedral Uranium(V) Complex. Inorganic Chemistry, 2018, 57, 8106-8115.	4.0	16
45	Backbone Dehydrogenation in Pyrrole-Based Pincer Ligands. Inorganic Chemistry, 2018, 57, 9544-9553.	4.0	16
46	Crystal structures of two new six-coordinate iron(III) complexes with 1,2-bis(diphenylphosphane) ligands. Acta Crystallographica Section E: Crystallographic Communications, 2018, 74, 803-807.	0.5	0
47	Multinuclear iron–phenyl species in reactions of simple iron salts with PhMgBr: identification of Fe4(μ-Ph)6(THF)4 as a key reactive species for cross-coupling catalysis. Chemical Science, 2018, 9, 7931-7939.	7.4	34
48	Transition-Metal-Free Formation of C–E Bonds (E = C, N, O, S) and Formation of C–M Bonds (M = Mn,) Tj ETG Organometallics, 2017, 36, 849-857.	Qq0 0 0 rg 2.3	BT /Overlock 12
49	Intermediates and Reactivity in Iron-Catalyzed Cross-Couplings of Alkynyl Grignards with Alkyl Halides. Journal of the American Chemical Society, 2017, 139, 6988-7003.	13.7	46
50	Polyoxovanadate–Alkoxide Clusters as a Redox Reservoir for Iron. Inorganic Chemistry, 2017, 56, 7065-7080.	4.0	48
51	A Physicalâ€Inorganic Approach for the Elucidation of Active Iron Species and Mechanism in Ironâ€Catalyzed Crossâ€Coupling. Israel Journal of Chemistry, 2017, 57, 1106-1116.	2.3	24
52	Magnetic circular dichroism and density functional theory studies of electronic structure and bonding in cobalt(ii)–N-heterocyclic carbene complexes. Dalton Transactions, 2017, 46, 13290-13299.	3.3	18
53	Iron(II) Complexes of a Hemilabile SNS Amido Ligand: Synthesis, Characterization, and Reactivity. Inorganic Chemistry, 2017, 56, 13766-13776.	4.0	22
54	Magnetic circular dichroism of UCl <sub>6</sub> <sup>â^'</sup> in the ligand-to-metal charge-transfer spectral region. Physical Chemistry Chemical Physics, 2017, 19, 17300-17313.	2.8	21

#	Article	IF	CITATIONS
55	A Combined Probe-Molecule, Mössbauer, Nuclear Resonance Vibrational Spectroscopy, and Density Functional Theory Approach for Evaluation of Potential Iron Active Sites in an Oxygen Reduction Reaction Catalyst. Journal of Physical Chemistry C, 2017, 121, 16283-16290.	3.1	75
56	Magnetic circular dichroism studies of iron( <scp>ii</scp> ) binding to human calprotectin. Chemical Science, 2017, 8, 1369-1377.	7.4	22
57	Catalytic Light-Driven Generation of Hydrogen from Water by Iron Dithiolene Complexes. Journal of the American Chemical Society, 2016, 138, 11654-11663.	13.7	96
58	Manipulating Magneto-Optic Properties of a Chiral Polymer by Doping with Stable Organic Biradicals. Nano Letters, 2016, 16, 5451-5455.	9.1	30
59	Resident holes and electrons at organic/conductor and organic/organic interfaces: An electron paramagnetic resonance investigation. Organic Electronics, 2016, 37, 379-385.	2.6	1
60	Magnetic Circular Dichroism and Density Functional Theory Studies of Iron(II)-Pincer Complexes: Insight into Electronic Structure and Bonding Effects of Pincer N-Heterocyclic Carbene Moieties. Organometallics, 2016, 35, 3692-3700.	2.3	14
61	Isolation, Characterization, and Reactivity of Fe <sub>8</sub> Me <sub>12</sub> <sup>–</sup> : Kochi's <i>S</i> = 1/2 Species in Iron-Catalyzed Cross-Couplings with MeMgBr and Ferric Salts. Journal of the American Chemical Society, 2016, 138, 7492-7495.	13.7	81
62	Facile hydrogen atom transfer to iron( <scp>iii</scp> ) imido radical complexes supported by a dianionic pentadentate ligand. Chemical Science, 2016, 7, 5939-5944.	7.4	47
63	Electronic Structure and Bonding in Iron(II) and Iron(I) Complexes Bearing Bisphosphine Ligands of Relevance to Iron-Catalyzed C–C Cross-Coupling. Inorganic Chemistry, 2016, 55, 272-282.	4.0	32
64	Mononuclear, Dinuclear, and Trinuclear Iron Complexes Featuring a New Monoanionic SNS Thiolate Ligand. Inorganic Chemistry, 2016, 55, 987-997.	4.0	23
65	Possible Demonstration of a Polaronic Bose-Einstein(-Mott) Condensate in UO2(+x) by Ultrafast THz Spectroscopy and Microwave Dissipation. Scientific Reports, 2015, 5, 15278.	3.3	13
66	Crystal structure of a third polymorph of tris(acetylacetonato-κ <sup>2</sup> <i>O</i> , <i>O</i> ′)iron(III). Acta Crystallographica Section E: Crystallographic Communications, 2015, 71, m228-m229.	0.5	8
67	How Innocent are Potentially Redox Non-Innocent Ligands? Electronic Structure and Metal Oxidation States in Iron-PNN Complexes as a Representative Case Study. Inorganic Chemistry, 2015, 54, 4909-4926.	4.0	76
68	Ambivalent binding between a radical-based pincer ligand and iron. Dalton Transactions, 2015, 44, 10516-10523.	3.3	15
69	Iron(II) Active Species in Iron–Bisphosphine Catalyzed Kumada and Suzuki–Miyaura Cross-Couplings of Phenyl Nucleophiles and Secondary Alkyl Halides. Journal of the American Chemical Society, 2015, 137, 11432-11444.	13.7	101
70	Linear and T-Shaped Iron(I) Complexes Supported by N-Heterocyclic Carbene Ligands: Synthesis and Structure Characterization. Inorganic Chemistry, 2015, 54, 8808-8816.	4.0	36
71	A combined magnetic circular dichroism and density functional theory approach for the elucidation of electronic structure and bonding in three- and four-coordinate iron( <scp>ii</scp> )–N-heterocyclic carbene complexes. Chemical Science, 2015, 6, 1178-1188.	7.4	44
72	Direct observation of ICT cations at the HTL/transparent semiconductor interface. Organic Electronics, 2014, 15, 3761-3765.	2.6	2

#	Article	IF	CITATIONS
73	Iron Dicarbonyl Complexes Featuring Bipyridineâ€Based PNN Pincer Ligands with Short Interpyridine CC Bond Lengths: Innocent or Nonâ€Innocent Ligand?. Chemistry - A European Journal, 2014, 20, 4403-4413.	3.3	56
74	Flexible Binding of PNP Pincer Ligands to Monomeric Iron Complexes. Inorganic Chemistry, 2014, 53, 6066-6072.	4.0	32
75	Reactivity of (NHC) <sub>2</sub> FeX <sub>2</sub> Complexes toward Arylborane Lewis Acids and Arylboronates. Organometallics, 2014, 33, 370-377.	2.3	25
76	Isolation and Characterization of a Tetramethyliron(III) Ferrate: An Intermediate in the Reduction Pathway of Ferric Salts with MeMgBr. Journal of the American Chemical Society, 2014, 136, 15457-15460.	13.7	61
77	Two- and three-coordinate formal iron( <scp>i</scp> ) compounds featuring monodentate aminocarbene ligands. Organic Chemistry Frontiers, 2014, 1, 1040-1044.	4.5	31
78	Iron Phosphine Catalyzed Cross-Coupling of Tetraorganoborates and Related Group 13 Nucleophiles with Alkyl Halides. Organometallics, 2014, 33, 5767-5780.	2.3	90
79	A Combined Mössbauer, Magnetic Circular Dichroism, and Density Functional Theory Approach for Iron Cross-Coupling Catalysis: Electronic Structure, In Situ Formation, and Reactivity of Iron-Mesityl-Bisphosphines. Journal of the American Chemical Society, 2014, 136, 9132-9143.	13.7	108
80	Covalency in f-element complexes. Coordination Chemistry Reviews, 2013, 257, 394-406.	18.8	415
81	Efficient Nazarov Cyclization/Wagner–Meerwein Rearrangement Terminated by a Cu <sup>II</sup> â€Promoted Oxidation: Synthesis of 4â€Alkylidene Cyclopentenones. Chemistry - A European Journal, 2013, 19, 4842-4848.	3.3	20
82	Activation of α-Keto Acid-Dependent Dioxygenases: Application of an {FeNO} <sup>7</sup> /{FeO <sub>2</sub> } <sup>8</sup> Methodology for Characterizing the Initial Steps of O <sub>2</sub> Activation. Journal of the American Chemical Society, 2011, 133, 18148-18160.	13.7	66
83	Mechanism of the Decomposition of Aqueous Hydrogen Peroxide over Heterogeneous TiSBA15 and TS-1 Selective Oxidation Catalysts: Insights from Spectroscopic and Density Functional Theory Studies. ACS Catalysis, 2011, 1, 1665-1678.	11.2	99
84	Ag K-Edge EXAFS Analysis of DNA-Templated Fluorescent Silver Nanoclusters: Insight into the Structural Origins of Emission Tuning by DNA Sequence Variations. Journal of the American Chemical Society, 2011, 133, 11837-11839.	13.7	78
85	Insight into contributions to phenol selectivity in the solution oxidation of benzene to phenol with H2O2. Catalysis Communications, 2011, 12, 480-484.	3.3	41
86	The Three-His Triad in Dke1: Comparisons to the Classical Facial Triad. Biochemistry, 2010, 49, 6945-6952.	2.5	44
87	Direct Observation of Acetyl Group Formation from the Reaction of CO with Methylated H-MOR by in Situ Diffuse Reflectance Infrared Spectroscopy. Journal of Physical Chemistry Letters, 2010, 1, 3012-3015.	4.6	17
88	Formation and Stabilization of Fluorescent Gold Nanoclusters Using Small Molecules. Journal of Physical Chemistry C, 2010, 114, 15879-15882.	3.1	88
89	Geometric Structure Determination of N694C Lipoxygenase: A Comparative Near-Edge X-Ray Absorption Spectroscopy and Extended X-Ray Absorption Fine Structure Study. Inorganic Chemistry, 2008, 47, 11543-11550.	4.0	7
90	VTVH-MCD and DFT Studies of Thiolate Bonding to {FeNO}7/{FeO2}8Complexes of IsopenicillinNSynthase:Â Substrate Determination of Oxidase versus Oxygenase Activity in Nonheme Fe Enzymes. Journal of the American Chemical Society, 2007, 129, 7427-7438.	13.7	105

#	Article	IF	CITATIONS
91	CD and MCD of CytC3 and Taurine Dioxygenase:  Role of the Facial Triad in α-KG-Dependent Oxygenases. Journal of the American Chemical Society, 2007, 129, 14224-14231.	13.7	86
92	Kinetic and Spectroscopic Studies of N694C Lipoxygenase:  A Probe of the Substrate Activation Mechanism of a Nonheme Ferric Enzyme. Journal of the American Chemical Society, 2007, 129, 7531-7537.	13.7	27
93	Kinetic, Spectroscopic, and Structural Investigations of the Soybean Lipoxygenase-1 First-Coordination Sphere Mutant, Asn694Glyâ€,‡. Biochemistry, 2006, 45, 10233-10242.	2.5	17
94	Spectroscopic and electronic structure studies of the role of active site interactions in the decarboxylation reaction of α-keto acid-dependent dioxygenases. Journal of Inorganic Biochemistry, 2006, 100, 2108-2116.	3.5	16
95	Spectroscopic and electronic structure studies of aromatic electrophilic attack and hydrogen-atom abstraction by non-heme iron enzymes. Proceedings of the National Academy of Sciences of the United States of America, 2006, 103, 12966-12973.	7.1	143
96	Structure–function correlations in oxygen activating non-heme iron enzymes. Chemical Communications, 2005, , 5843.	4.1	90
97	Spectroscopic and computational studies of NTBC bound to the non-heme iron enzyme (4-hydroxyphenyl)pyruvate dioxygenase: Active site contributions to drug inhibition. Biochemical and Biophysical Research Communications, 2005, 338, 206-214.	2.1	28
98	CD and MCD Studies of the Non-Heme Ferrous Active Site in (4-Hydroxyphenyl)pyruvate Dioxygenase:Â Correlation between Oxygen Activation in the Extradiol and α-KG-Dependent Dioxygenases. Journal of the American Chemical Society, 2004, 126, 4486-4487.	13.7	60
99	Spectroscopic Characterization of Soybean Lipoxygenase-1 Mutants:  the Role of Second Coordination Sphere Residues in the Regulation of Enzyme Activity. Biochemistry, 2003, 42, 7294-7302.	2.5	49
100	A TMEDAâ€Iron Adduct Reaction Manifold in Ironâ€Catalyzed C(sp2)â€C(sp3) Crossâ€Coupling Reactions. Angewandte Chemie, 0, , .	2.0	0